

Phase diagram of the heavy fermion system YbFe_2Ge_2 under pressure

J. Larrea J.,¹ M. B. Fontes,¹ E. M. Baggio-Saitovitch,¹ J. Plessel,² M. M. Abd-Elmeguid,² J. Ferstl,³ C. Geibel,³ A. Pereira,⁴ A. Jornada,⁴ and M. A. Continentino^{5,*}

¹*Centro Brasileiro de Pesquisas Físicas, Rua Xavier Sigaud, Rio de Janeiro, RJ, Brazil*

²*II. Physikalisches Institut, Universität zu Köln, Zùlpicher Strasse 77, 50937 Köln, Germany*

³*Max-Planck Institute for Chemical Physics of Solids, D-01187 Dresden, Germany*

⁴*Instituto de Física, Universidade Federal do Rio Grande do Sul, Brazil*

⁵*Instituto de Física, Universidade Federal Fluminense, Campus da Praia Vermelha, Niterói, 24210-340, RJ, Brazil*

(Received 23 December 2005; published 27 October 2006)

The phase diagram of the heavy fermion compound YbFe_2Ge_2 under high pressures $P \leq 18.2$ GPa was obtained by electrical resistivity measurements. Pressure drives the system from a paramagnetic Fermi liquid state to a magnetically ordered state, with a quantum critical point at $P_C \approx 9.4$ GPa. In the vicinity of P_C a non-Fermi-liquid behavior ascribed to two-dimensional antiferromagnetic fluctuations is observed. In the magnetic side, the resistivity shows the existence of spin-wave excitations characteristic of an antiferromagnet.

DOI: [10.1103/PhysRevB.74.140406](https://doi.org/10.1103/PhysRevB.74.140406)

PACS number(s): 71.27.+a, 62.50.+p, 71.10.Hf, 72.10.Di

The study of the ground-state properties of strongly correlated f -electron systems such as heavy fermions (HF's)—e.g., Ce-, U-, or Yb-based intermetallic compounds—is one of the most attractive topics in modern condensed matter physics. Of particular interest is the investigation of HF systems under high pressure that are close to the borderline between the magnetically ordered and nonmagnetic ground states—i.e., close to a magnetic quantum critical point (QCP).¹ This is related to the fact that critical fluctuations in the vicinity of a QCP strongly affect the physical properties of the system and result in non-Fermi-liquid (NFL) behavior and the formation of new ground states² including unconventional superconductivity and novel phenomena.^{3–7}

Despite the great number of magnetic Ce- and U-based HF materials studied close to a QCP, few examples of quantum criticality in nonmagnetic (NM) Yb-based HF compounds under pressure experiments¹ have been reported. This is due to the scarcity of clean Yb HF compounds and/or because such compounds require very large pressures to achieve a magnetically ordered (MO) state. In the latter case the thermodynamics characterization of the induced magnetic QCP at the critical pressure (P_C) is nonfeasible, at present.⁸ Instead of P , an external magnetic field B has been recently used as a control parameter to study a field-induced QCP in antiferromagnetic (AF) Yb HF systems,¹ despite only a few cases having been reported.^{9,10} More recently, Mössbauer experiments under high pressures on YbRh_2Si_2 showed a first-order transition (FOT), from a low-moment (LM) to a high-moment (HM) state, at $P_T \sim 10$ GPa,¹¹ and a similar FOT was reported in YbAgGe .¹² Therefore, the discovery of a new Yb-based HF and its study under pressure may give important contributions to the understanding of the quantum criticality in HF's.

The recently discovered HF material YbFe_2Ge_2 with a paramagnetic Fermi liquid (FL) ground state at ambient pressure ($P=0$) is a promising candidate for the study of the quantum critical region of the phase diagram. It crystallizes in a tetragonal ThCr_2Si_2 -type structure with lattice parameters: $a=3.924$ Å and $c=10.503$ Å.¹³ Previous susceptibility $\chi(T)$ and specific heat $C(T)$ measurements on this compound revealed a NM state with a broad maximum in $\chi(T)$ around

15 K and $C(T) = \gamma T + \beta T^3$ below 20 K with $\gamma = 200$ mJ mol⁻¹ K⁻². These results point to a nonmagnetic Fermi liquid state with a characteristic $4f$ energy of ~ 75 K, characterizing this compound as a moderate HF system at the border between the Kondo and the intermediate valence regime.¹³ In this Rapid Communication we report the phase diagram obtained from high-pressure electrical resistance measurements on a stoichiometric polycrystalline YbFe_2Ge_2 sample.

Small pieces were prepared out of the polycrystalline batches, as reported in Ref. 13. Powder XRD diffraction confirmed these samples to be single phase. The large residual resistivity $\rho_0 \approx 60$ $\mu\Omega$ cm, despite a rather good resistivity ratio $\text{RRR} \approx 8$, might be due to the presence of poorly conducting grain boundaries. Electrical resistance measurements under P have been performed using the same type of diamond anvil cell (DAC) described in Ref. 14, with a standard four-probe method and $P \leq 18.2$ GPa. They were performed with two different batches of sample for the same DAC setup and reproduced quite similar results. The resistivity $\rho(T)$ was estimated assuming a van der Pauw geometry. A ³He-⁴He dilution refrigerator was used to measure the electrical resistance down to 0.05 K. An epoxy reinforced with Al_2O_3 is used as P -transmitting medium. Pressures were determined by the induced shift of the $R1$ fluorescence line of ruby, and its distribution in the cell guarantees quasihydrostatic P conditions in our experiments ($\leq 10\%$).

Figure 1 shows the temperature dependence of the normalized electrical resistance curves $R/R(295\text{ K})$ for YbFe_2Ge_2 at different pressures. A zoom-in of the low-temperature data ($T < 20$ K) is shown in the inset of Fig. 1. It reveals the presence of kinks at temperatures T_N around $\approx 1\text{--}3$ K for $P \geq 11$ GPa (Fig. 1) which become more clearly defined at higher P (inset of Fig. 1). These kinks are the signature of^{8–12,15,16} the onset of a magnetically ordered state as discussed below.

The $\Delta\rho(T) = \rho - \rho_0 \propto T^\varepsilon$ dependence of the electrical resistivity shows distinct behavior at different ranges of T . From the lowest T to an upper limit T_{coh} , the coherence temperature [Fig. 2(a)], $\varepsilon=2$ characterizes a FL state for all $P \leq 8.9$ GPa.³ As shown in Fig. 3, T_{coh} decreases with P and

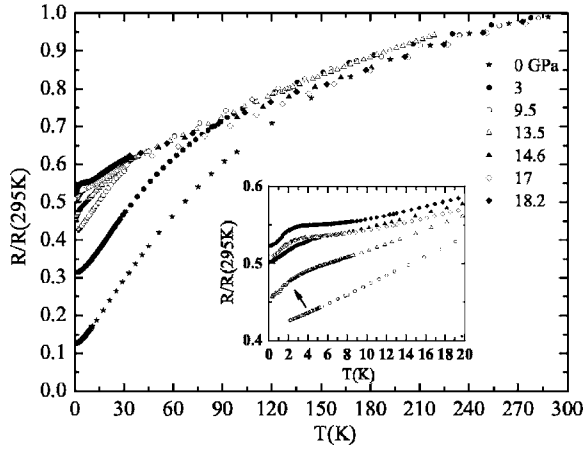


FIG. 1. Temperature dependence of the electrical resistance for YbFe_2Ge_2 compound, at the indicated pressures, normalized to the resistance value at 295 K. The inset shows a zoom-in for selected pressures at temperatures $T < 20$ K. The arrow indicates the onset of the magnetic ordering state.

seems to vanish at the pressure $P_0=9.4(2)$. Assuming that the coherence line is described by a critical and an analytic contribution, $(P-P_0)=|-a(T_{coh})^2-b(T_{coh})^{z/2}|$, where z is the dynamic exponent,³⁻⁶ T_{coh} increasing almost linearly with $P-P_0$ implies $z=2$. This is confirmed by a fit using the complete equation. The resulting solid line in Fig. 3 fits the ex-

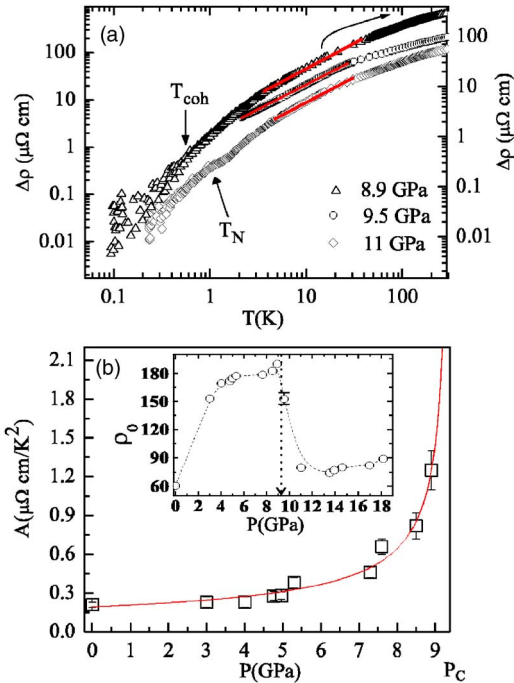


FIG. 2. (Color online) (a) Logarithmic plot of $\Delta\rho(T)$, where the solid lines show the $T^{1.0(1)}$ dependence over more than one decade in T associated with a NFL behavior. The arrows indicate the onset of the FL behavior (T_{coh}) and the magnetic ordering state (T_N). (b) P dependence of A , the QP-QP scattering cross section. The solid line represents $|P-P_0|^{-0.6(1)}$. Inset: P dependence of the residual resistivity ρ_0 ; the dashed line indicates the pressure where ρ_0 starts to decrease ~ 9.5 GPa.

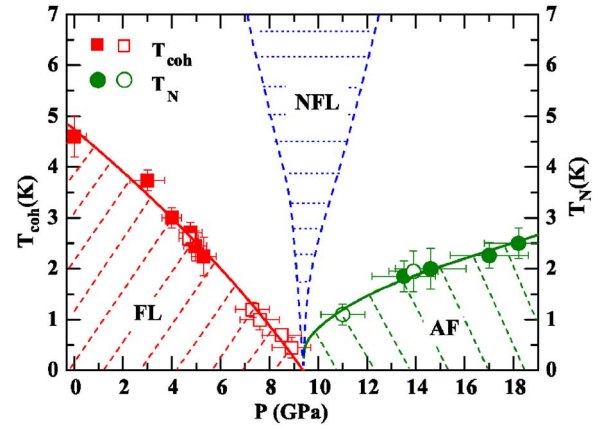


FIG. 3. (Color online) Suggested phase diagram for YbFe_2Ge_2 . Open and solid symbols represent two different pressure runs. The solid lines are fits to $T_{coh}(P)$ using both mean-field and true critical contributions (see text) and to $T_N(P)$ considering 2D-AF spin-wave gaps with a QCP at $P_C \sim 9.4$ GPa (see text). NFL regime with $\varepsilon = 1.0(1)$ is also shown.

perimental data very nicely. The result $z=2$ suggests that YbFe_2Ge_2 is close to an AF instability.^{4,6}

In the FL state, the P dependence of the coefficient A , such that $A=\Delta\rho/T^2$, gives relevant information about the nature of criticality. Figure 2(b) shows the values of the obtained $A(P)$. The ratio $A/\gamma^2=0.5 \times 10^{-5} \mu\Omega \text{ cm} (\text{mol K mJ}^{-1})^2$, taken from $P=0$ data, is typical of HF's with the degeneracy of quasiparticles (QP's) $N=2$; i.e., most of the degeneracy is lost because of the large crystal-field splitting Δ' .¹⁷ The values of $A(P)$ exhibit a pronounced increase from 5 GPa up to pressures close, but below, P_0 and can be fitted by $A(P) \propto |P-P_0|^{-n}$, with $n=0.6(1)$. This value is in agreement with the spin fluctuation (SF) theory ($n=0.5$) for a system in the nonlocal critical regime of the AF-QCP.^{3,18} Since YbFe_2Ge_2 behaves as a true FL for $P < P_0$ and $T < T_{coh}$, the behavior of $A(P)$ in Fig. 2(b) indicates that the whole Fermi surface undergoes singular scattering at P_0 .^{18,19}

Another piece of evidence of QCP is shown in Fig. 2(a), where NFL behavior is found for P close to P_0 and above some characteristic temperature T_{coh} or $T_N(P)$ —i.e., in the NM and magnetic (M) sides of the phase diagram. An exponent $\varepsilon=1.0(1)$ is valid over more than one decade in T . The exponent $\varepsilon=1$ generally indicates the presence of two-dimensional (2D) AF spin fluctuations at the QCP.^{8,19} The fact that the NFL behavior is larger at 9.5 GPa (at least down to 2 K) reinforces the argument that the QCP should be located close to $P_0 \approx 9.4$ GPa.

The inset of Fig. 2(b) shows the P dependence of the residual resistivity $\rho_0(P)$, which was estimated from the average value of the resistivity between $T \sim 0.1$ and 0.2 K for all pressures except for the case of $P=9.5$ GPa, where a linear extrapolation down to $T=0$ was done. The error bars in ρ_0 are rather small even in the case of $P=9.5$ GPa. A broad maximum of $\rho_0(P)$ is observed in the FL regime, with a clear reduction in ρ_0 as approaching 9.5 GPa. This trend of $\rho_0(P)$ has been reported in other Yb-based HF's.^{15,16,20} The peak in

$\rho_0(P)$ occurs close to the critical pressure with the appearance of magnetic order and reveals the presence of charge (valence) fluctuations, as discussed below. One can argue that the YbFe_2Ge_2 system belongs to the class of materials where P may induce a valence change towards a magnetic Yb^{3+} state.¹⁶ Therefore the existence of a magnetic QCP, close to $P_0=9.4$ GPa, is consistent with the $\rho_0(P)$ profile. The downturn of $\rho_0(P)$ at 9.5 GPa suggests that most of the magnetic moments are already ordered at that pressure. In the following, we show an approach that takes into account spin waves (SW's) in the magnetically ordered phase, which allows us to infer from our data the existence of a magnetic QCP at $P_C \approx 9.4$ GPa.

A clear indication of magnetic ordering are the kinks in the $\rho(T)$ curves for $P \geq 11$ GPa [inset of Figs. 1 and 2(a)] which can be identified as T_N . The increase of T_N with P indicates that YbFe_2Ge_2 develops a long-range-ordered magnetic state, possibly AF, out of the QCP. So, other aspects about quantum criticality can be inferred in the magnetic phase, above 11 GPa and below $T_N(P)$. The low-energy magnetic excitations (magnons or spin waves) scatter the conduction electrons, giving rise to a magnetic contribution $\rho_m(T)$ to the resistivity that is usually obtained by subtracting the phonon contribution $\rho_{ph}(T)$. Since the latter can be safely neglected in the YbFe_2Ge_2 sample below $T_N(P)$,²¹ the magnetic resistivity data at low temperatures are given by $\rho_m(T) = \rho_0 + \rho_{SW}(T) + mT^n$. ρ_{SW} is the SW contribution, and the second term mT^n , with $1 < n \leq 2$, takes into account electron-electron (ee) scattering.^{19,22–25} In anisotropic antiferromagnets, the dispersion relation of the hydrodynamic spin-wave modes is given by $\omega(k) = \sqrt{\Delta^2 + Dk^2}$, where Δ is the SW gap and D the SW stiffness. The magnon gap is due to the magnetic anisotropy arising from the peculiarities of the induced magnetic structure of YbFe_2Ge_2 and the high anisotropy of the electronic f states.^{13,25} For $k_B T < \Delta$, one finds, for $\rho_{SW}(T)$,²⁶

$$\rho_{SW} = C \left(\frac{\Delta}{k_B} \right)^{3/2} T^{1/2} e^{-\Delta/k_B T} \left[1 + \frac{2}{3} \left(\frac{k_B T}{\Delta} \right) + \frac{2}{15} \left(\frac{k_B T}{\Delta} \right)^2 \right], \quad (1)$$

where the coefficient C is related to the spin-wave stiffness by $D \propto 1/C^{2/3}$ or $\Gamma \propto 1/C^{1/3}$, where Γ is the effective magnetic coupling between Yb ions.

The resistivity data were fitted in the range of temperature $T_{fit} \leq 0.55T_N$ [Fig. 4(a)], where ρ_0 is taken as the only fixed parameter in the fit. One can see—for instance, at $P = 18.2$ GPa—that the spin-wave contribution to $\rho_m(T)$ is dominant. This guarantees that the values obtained for the gap Δ and the parameter C from the fits are quite reliable. Figure 4(b) shows the pressure dependence of the gap $\Delta(P)$, the stiffness $D(P)$, and $T_N(P)$. There is a clear correlation between $T_N(P)$ and $\Delta(P)$. Both increase with pressure, showing a developing of the MO state as YbFe_2Ge_2 moves away from the QCP. In particular, the gap increases linearly with pressure and faster than T_N and an extrapolation of $\Delta/k_B \rightarrow 0$ K yields the same critical pressure as before $P_C \approx 9.4$ GPa.

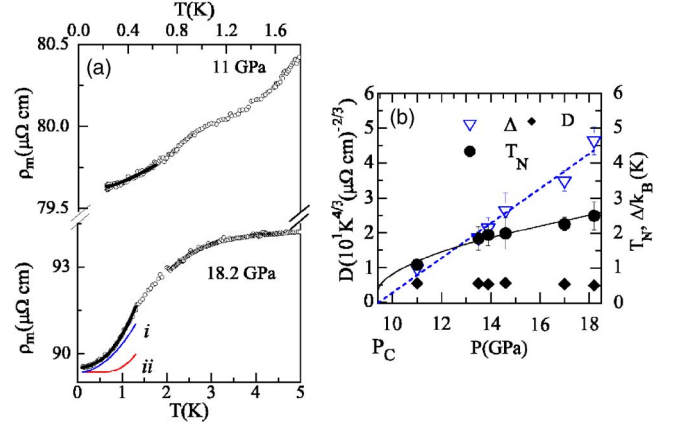


FIG. 4. (Color online) (a) Magnetic contribution to the resistivity, $\rho_m(T)$, of YbFe_2Ge_2 , where solid lines are the fits using Eq. (1). At $P = 18.2$ GPa, the curves labeled with i and ii correspond to SW and ee scattering (with $n=2$) contributions, respectively (see text). (b) Pressure dependence of Δ , D , and T_N parameters for $P > 11$ GPa. The solid line is obtained from Eq. (2) considering a gap Δ described by the dashed line and $\Gamma/k_B \sim 2.42$ K (see text).

It is remarkable in Fig. 4(b) that the bare spin-wave stiffness $D(P)$ remains nearly unchanged, and probably finite down to P_C . In this way, the disappearance of T_N as the QCP is approached can not be explained only by a softening of the spin waves. Within the spin-wave approach this can occur if the magnetic excitations are two dimensional and, in agreement with the experiments, they become isotropic at the QCP. In this case the vanishing of the spin-wave gap at P_C drives the magnetic instability. This scenario was previously proposed to describe the AF-QCP and FM-QCP transitions for $\text{CeCoGe}_{2.25}\text{Si}_{0.75}$ (Ref. 26) and CePt (Ref. 25), respectively. Continentino *et al.*²⁶ obtained an expression which relates $T_N(P)$ with $\Delta(P) \propto |\delta| = |P - P_C|$ is taken as a control parameter. For a $d=2$ system there is long-range order at finite temperatures only in the presence of a spin-wave gap. The critical temperature ($S=1/2$) is given by

$$k_B T_N = \frac{2\Gamma}{\sqrt{1 + (\Delta/\Gamma)^2} \ln \left[1 + \frac{\pi^2}{2(\Delta/\Gamma)^2} \right]}. \quad (2)$$

and $T_N \rightarrow 0$ when $\Delta \rightarrow 0$. So choosing a pressure range where $D(P)$ is nearly constant and since $\Gamma \propto \sqrt{D}$ and $\Delta(P) = 0.4966|P - 9.4|$ as obtained from the ρ_m data, the only free adjustable parameter to fit in Eq. (2) is Γ . This yields $\Gamma/k_B = 2.42$ K, a value comparable with Γ values for other HF's with magnetic-QCP transitions.^{25,26} As shown in Fig. 4(b), the critical line $T_N(P)$ is reproduced even far from the QCP. Since our results for $T_N(P)$ can be described by Eq. (2), the present mechanism of soft gap and two-dimensional magnetic excitations gives a plausible and consistent explanation of the quantum criticality of YbFe_2Ge_2 on the ordered magnetic phase.

Equation (2) is obtained with the assumption that the local magnetic moments of Yb remain unquenched down to the QCP. This is consistent with neutron scattering in the mirror

systems CeRh_2Si_2 (Ref. 23) or $\text{CeCu}_{6-x}\text{Au}_x$ (Ref. 27) that show the presence of local magnetic moments of Ce ions even at the QCP. Moreover, the two-dimensional character of magnetic excitations is in agreement with the tetragonal crystalline structure of YbFe_2Ge_2 , in which the antiferromagnetic layered squares may be frustrated along the c axis.

In conclusion, the analysis of the $\rho(T)$ data classifies YbFe_2Ge_2 as a new HF material where pressure induces NM-M quantum phase transition with a QCP at $P_C \approx 9.4(4)$ GPa. The inferred quantum criticality of YbFe_2Ge_2 belongs to the same universality class of those systems found in the nonlocal critical regime of AF-QCP. The P -induced non-Fermi-liquid behavior seen as $\rho(T) \propto T$ reinforces the idea that YbFe_2Ge_2 is driven towards AF instability. At the magnetic side, we can clearly see in our phase diagram that an usual linear extrapolation of $T_N(P)$ to obtain P_C is inconsistent. Since our $\rho_m(T)$ data can be well described by AF spin waves, we can adopt a model, where two-dimensional magnons become isotropic or gapless at P_C , giving rise to a magnetic instability at the same pressure. This model successfully accounts for our experimental results and even allows us to obtain a numerical value for the bare exchange interaction between the unquenched local moments along the

relevant planes in the ordered magnetic phase of YbFe_2Ge_2 . The model also describes quite well the weak pressure dependence of $T_N(P)$ on the MO side, which looks different from the usual Doniach's diagram. As recently reported by Plessel *et al.*¹¹ for an isostructural YbRh_2Si_2 compound, this smooth increase of T_N can be understood using a scenario where dynamical two-dimensional SF act on the LM state.¹² This reinforces the idea that the 2D critical fluctuations are the main driving force to account for the criticality of YbFe_2Ge_2 . It would be very useful to perform neutron scattering in magnetically ordered heavy fermions²⁸ to confirm the behavior with pressure of the spin-wave parameters.¹⁹ Also local probe Yb spectroscopy^{11,15,16} could help to elucidate the importance of valence fluctuations close to a magnetic QCP.

We thank H. Micklitz for helpful discussions and R. Lengsdorf for assistance in the DAC setup. Support for this collaboration by CAPES, CNPq, FAPERJ, and DAAD is gratefully acknowledged. Work partially supported by PRONEX/MCT and FAPERJ/Cientista do Nosso Estado programs.

*Electronic address: jlarrea@cbpf.br

- ¹For a review see G. R. Stewart, *Rev. Mod. Phys.* **73**, 797 (2001).
- ²C. Pfleiderer, D. Reznik, L. Pintschovius, H. V. Löhneysen, M. Garst, and A. Roch, *Nature (London)* **427**, 227 (2004).
- ³M. A. Continentino, G. M. Japiassu, and A. Troper, *Phys. Rev. B* **39**, 9734 (1989).
- ⁴A. J. Millis, *Phys. Rev. B* **48**, 7183 (1993).
- ⁵J. A. Hertz, *Phys. Rev. B* **14**, 1165 (1976).
- ⁶T. Moriya and T. Takimoto, *J. Phys. Soc. Jpn.* **64**, 3, 960 (1995).
- ⁷A. H. Castro Neto, G. Castilla, and B. A. Jones, *Phys. Rev. Lett.* **81**, 3531 (1998).
- ⁸O. Trovarelli, C. Geibel, S. Mederle, C. Langhammer, F. M. Grosche, P. Gegenwart, M. Lang, G. Sparn, and F. Steglich, *Phys. Rev. Lett.* **85**, 626 (2000).
- ⁹J. Custers, P. Gegenwart, H. Wilhelm, K. Neumaier, Y. Tokiwa, O. Trovarelli, C. Geibel, F. Steglich, C. Pépin, and P. Coleman, *Nature (London)* **424**, 524 (2003).
- ¹⁰S. L. Bud'ko, E. Morosan, and P. C. Canfield, *Phys. Rev. B* **69**, 014415 (2004); P. G. Niklowitz, G. Knebel, and J. Flouquet, *ibid.* **73**, 125101 (2006).
- ¹¹J. Plessel, M. M. Abd-Elmeguid, J. P. Sanchez, G. Knebel, C. Geibel, O. Trovarelli, and F. Steglich, *Phys. Rev. B* **67**, 180403(R) (2003).
- ¹²K. Umeo, K. Yamane, Y. Muro, K. Katoh, Y. Niide, A. Ochiai, and T. Takabatake, *Physica B* **359**, 130 (2005).
- ¹³J. Ferstl and C. Geibel (private communication).
- ¹⁴E. N. Van Eenige, R. Griessen, R. J. Wijngaarden, J. Karpinski, E. Kaldis, S. Rusiecki, and E. Jilek, *Physica C* **168**, 482 (1990).
- ¹⁵H. Winkelmann, M. M. Abd-Elmeguid, H. Micklitz, J. P. Sanchez, C. Geibel, and F. Steglich, *Phys. Rev. Lett.* **81**, 4947 (1998).
- ¹⁶H. Winkelmann, M. M. Abd-Elmeguid, H. Micklitz, J. P. Sanchez, P. Vulliet, K. Alami-Yadri, and D. Jaccard, *Phys. Rev. B* **60**, 3324 (1999).

- ¹⁷N. Tsujii, H. Kontani, and K. Yoshimura, *Phys. Rev. Lett.* **94**, 057201 (2005).
- ¹⁸M. A. Continentino, *Quantum Scaling in Many-Body Systems, Lecture Notes in Physics*, Vol. 67 (World Scientific, Singapore, 2001).
- ¹⁹P. Gegenwart, J. Custers, C. Geibel, K. Neumaier, T. Tayama, K. Tenya, O. Trovarelli, and F. Steglich, *Phys. Rev. Lett.* **89**, 056402 (2002).
- ²⁰D. Jaccard, H. Wilhelm, K. Alami-Yadri, and E. Vargoz, *Physica B* **259–261**, 1 (1999).
- ²¹From H. Wilhelm and D. Jaccard, *Phys. Rev. B* **66**, 064428 (2002), $\rho_{ph}(T) \approx 0.1 \mu\Omega \text{ cm/K T}$. Then at $T=3$ K, $\rho_{ph} \sim 0.3 \mu\Omega \text{ cm}$ and $\rho_0(\text{YbFe}_2\text{Ge}_2) \geq 60 \mu\Omega \text{ cm}$.
- ²²N. D. Mathur, F. M. Grosche, S. R. Julian, I. R. Walker, D. M. Freye, R. K. W. Haselwimmer, and G. G. Lonzarich, *Nature (London)* **394**, 39 (1998).
- ²³T. T. M. Palstra, A. A. Menovsky, and J. A. Mydosh, *Phys. Rev. B* **33**, 6527 (1986).
- ²⁴A. Demuer, D. Jaccard, I. Sheikin, S. Raymond, B. Salce, J. Thomasson, D. Braithwaite, and J. Flouquet *J. Phys.: Condens. Matter* **13**, 9335 (2001).
- ²⁵J. Larrea J., M. B. Fontes, A. D. Alvarenga, E. M. Baggio-Saitovitch, T. Burghardt, A. Eichler, and M. A. Continentino, *Phys. Rev. B* **72**, 035129 (2005).
- ²⁶M. A. Continentino, S. N. de Medeiros, M. T. D. Orlando, M. B. Fontes, and E. M. Baggio-Saitovitch, *Phys. Rev. B* **64**, 012404 (2001).
- ²⁷A. Schröder, G. Aeppli, R. Coldea, M. Adams, O. Stockert, H. V. Löhneysen, E. Bucher, R. Ramazashvili, and P. Coleman, *Nature (London)* **407**, 351 (2000); Q. Si, S. Rabello, K. Ingersent, and J. L. Smith, *ibid.* **413**, 804 (2001).
- ²⁸W. Knafo, S. Raymond, B. Fåk, G. Lapertot, P. C. Canfield, and J. Flouquet, *J. Phys.: Condens. Matter* **15**, 3741 (2003).